# The electronic structure and physicochemical characteristics of chlorohydroquinone compounds using density functional theory and Hartree-Fock techniques

**Bast Ahmed Mohammed[1], Rebaz Obaid Kareem[1]*, Othman Abdulrahman Hamad[2] and Hanifi Kebiroglu[3]**

[1]*Physics Department, College of Science, University of Halabja, Halabja, Iraq*
[2]*University of Raparin, College of Science, Department of Chemistry, Sulamani, Iraq*
[3]*Department of Opticianry, Darende Bekir Ilicak Vocational School, Malatya Turgut Ozal University, Malatya, Türkiye*

## ABSTRACT

**In the present research, the computer program Gaussian 5.0.9W was used to perform all calculations and physicochemical characteristics of 2-chlorobenzene-1,4-diol, 2,5-dichlorobenzene-1,4-diol, and 2,3,5,6-tetrachlorobenzene-1,4-diol molecules. The novelty of the work lies in the application of quantum computing analysis, specifically employing density functional theory (DFT) and Hartree-Fock (HF) techniques with a variety of basis sets (3-21G, 6-31G and 6-311G) to study the structure and characteristics of title compounds. In the current investigation, the influence of an increasing concentration of Cl compound on the electronegativity, dipole moment, and ionization potential was investigated. The following quantum chemical properties were derived: $E_{HOMO}$-$E_{LUMO}$ energy band gap (BG), energy ground state, ultraviolet (UV) spectroscopy, molecule electrostatic potential (MEP) on surfaces, density of states (DOS), reduced density gradient (RDG), nuclear magnetic resonance (NMR) including ground state energy E (B3LYP), thermodynamic parameters including thermal energy (E), entropy (S), molar heat capacity (Cv). Using a 6-31G basis set for DFT, the maximum amount of BG energy that can be transferred between HOMO and LUMO in a 2-chlorobenzene-1,4-diol molecule is 5.46 eV. Finally, based on our findings, the HF technique has a larger energy gap than the DFT approach. According to this, chlorohydroquinone compounds are less stable when using the DFT method, which suggests a higher degree of chemical reactivity.**

## KEYWORDS

**Chlorohydroquinone, DFT, Hartree-Fock method, HOMO-LUMO, NMR shielding, UV spectroscopy**

Received 7 August 2023, revised 8 February 2024, accepted 8 March 2024

## INTRODUCTION

Chlorophenols have a benzene ring, a -OH group, and one or more chlorine atoms attached to the ring.[1] The phenyl (Ph) rings, OH and Cl groups are ortho- and para-position concerning each other, so the electrophilic group radical attacks the electron-rich locations at the ortho- and para-sites.[2-4] One of the major byproducts of chlorophenol's photocatalytic breakdown is chlorohydroquinone. During the process chlorohydroquinone ($H_2QCl$) is photolyzed to hydroquinone ($QH_2$) and chlorobenzoquinone (QCl) in the air- or nitrogen-free solution. Then inverse reaction occurs, $QH_2$ is produced and photolyzed to form $H_2QCl$.[5] More than that, further oxidation of this QCl and other hydroxylated products through decarboxylation, and breaks the aromatic rings, resulting in acetic acid, maleic and fumaric acids.[4,6]

$H_2QCl$ is a chemical compound that has been utilized as an aromatic agent. It is a white crystalline solid that dissolves in water, alcohol, and ether. $H_2QCl$ is called 2-chlorohydroquinone-1,4-diol and 2-chloro-1,4-dihydroxybenzene, as shown in Figure 1,[7] and has the chemical formula is $C_6H_5ClO_2$ with a molecular weight of 144.55 g $mol^{-1}$, therefore the Mass-Charge Ratio (m/z) is 143.[8-9] $H_2QCl$ is a Ph molecule utilized as an intermediary in several organ chemical industries, posing a major hazard to the natural environment.[7] They are used in plastics, pesticides, and research laboratories. It is a persistent and hazardous organic molecule when it gets into the water supply.[10] Furthermore, it has several applications fungicide, developmental agent, and pharmacological intermediates. As $H_2QCl$ becomes more widely used, its potential for leakage into natural water rises, and even in low quantities, it may have devastating consequences on the biological environment.[7]

The toxicity and environmental durability of halo-hydrocarbons may be traced back to the stability of their C-Cl bond.[11] Due to the high electronegativity of the C-Cl bond to cleave requires about 525 kJ $mol^{-1}$ energy.[8] Also, three different conformations of chlorohydroquinone are possible, denoted by the letters TC, CC, TT, and CT in: the first letter means trans (T) or cis (C) hydroquinone, and the second letter denotes trans (T) or cis (C) conformation around the H-O-C=C-Cl part, because of the intramolecular hydrogen connection between the O-H and C-Cl groups, the optimal geometry for TC and CC is more stable than that for TT and CT, with computed relative energies of 0, 0.47, 12.6, and 13.5 kJ $mol^{-1}$ for TC, CC, TT, and CT respectively [12]. The hydrogen-bond stabilization energy is similar to 2-chlorophenol (13.1 kJ $mol^{-1}$).[13]

$QH_2$ and $H_2QCI$ have different pKa values, 10.2 and 8.6, respectively. This proves that $H_2QCI$ is more acidic than $QH_2$ . Although, the rate law for ($ClH_2Q$) in aqueous acidic solutions has been shown to rely on the oxidant and the reductant in a first-order fashion.[14-15] There is an accumulation of chloride ions in the medium reactions and the presence of $H_2QCI$ and $QH_2$. $H_2QCI$ also exhibits vibrations at 3325 $cm^{-1}$ for OH stretching, 1470 $cm^{-1}$ for C-H scissoring, and 743 $cm^{-1}$ for C-Cl stretching.[16-17]

$H_2QCl$, a degradation intermediate, commonly coexists with its isomers, including 2-chlorresorcinol and 4-chlorresorcinol, in environmental samples, making an accurate measurement of $H_2QCl$ difficult. However, tuning the band positions of carbon quantum dots (CQDs) experimentally is challenging because many factors, such as size and shape, control the HOMO and LUMO levels of CQDs, and

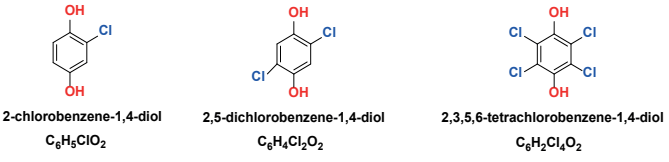


**Figure 1.** Three major structures of chlorohydroquinone compound using Chemdraw

*To whom correspondence should be addressed
Email: rebaz.kareem@uoh.edu.iq

ISSN 1996-840X Online / South African Chemical Institute / http://saci.co.za/journal

https://doi.org/10.17159/0379-4350/2024/v78a12

many of these cannot be precisely adjusted. We need an easy, reliable analytical approach for the sensitive, selective detection of $ClH_2Q$ as soon as possible. The most common techniques for determining $H_2QCl$ at this time are high-performance liquid chromatography (HPLC), gas chromatography-mass spectrometry (GC-MS), liquid chromatography-mass spectrometer (LC-MS), and HPLC/quadrupole time-of-flight/mass spectrometry (HPLC/Q–TOF/MS). These techniques are labor- and time-intensive, not to mention expensive. The direct and quick detection of $ClH_2Q$ is currently not easily achieved.[7]

In the context of this study, these properties are essential for understanding the structure-function relationships of molecules, predicting their behavior in various environments, designing new materials with specific properties, and advancing fields such as drug discovery, materials science, and chemical synthesis of chlorohydroquinone compounds. Investigating these properties in chlorohydroquinone compounds using density functional theory (DFT) and Hartree-Fock (HF), the research contributes to the fundamental understanding of molecular behavior of chlorohydroquinone and provides insights that can be applied across different scientific disciplines.

## COMPUTATIONAL STUDY

In the current investigation, the computer program Gaussian 5.0.9W was used to carry out all the essential atomic calculations and simulations in the three-dimensional shape of the molecule components while they were in the gas phase.[18] The computational chemistry software Gaussian 09W is accompanied with the graphical user interface GaussView 5.0. Therefore, GaussView 5.0 is a valuable tool for preparing, running, and analyzing Gaussian calculations in the field of computational chemistry. Further, the Gaussian 09W was employed for output calculations using HF and DFT techniques. Also, the DFT approach may give output data for more accurate estimates of complicated electrical characteristics since it considers electron density.[18-19] In addition, DFT is one of the significant methodologies that have shown a significant benefit over the Hartree-Fock method.[20] DFT and Hartree-Fock method were used in this examination to determine the HOMO, and LUMO states of 2-chlorobenzene-1,4-diol, 2,5-dichlorobenzene-1,4-diol, and 2,3,5,6-tetrachlorobenzene-1,4-diol compounds utilizing a variety of base sets, including 6-31G, 6-311G, and 3-21G, to determine the band gap (BGs) of the compound. The results of this calculation are presented in this paper. Using shape-optimized structures, groups of electrical characteristics were observed, such as total energy (E), electronegativity (χ), dipole moment (Debye), softness (S), hardness (H), chemical potential (Pi), and electrophilicity (ω) were all calculated.[21] For NMR, RDG, UV, PEM, DOS, and UV calculation we used the B3LYP level of theory (method) with a 3-21G basis set. Contributing same basis set is a more cohesive and comprehensive understanding of the physicochemical characteristics of the chlorohydroquinone compounds.

## RESULTS AND DISCUSSIONS

### Geometry optimization

In this section, the molecular structures were optimized, and the influence that solvents have on the relevant thermodynamic coefficients using the quantum mechanical method at the B3LYP for the optimized 2-chlorobenzene-1,4-diol, 2,5-dichlorobenzene-1,4-diol, and 2,3,5,6-tetrachlorobenzene-1,4-diol molecules as shown below Figure 2. However, to optimize our compounds, DFT and Hartree-Fock method have been used in this work. An advantageous way for optimizing the geometry of this approach begins by determining the energy associated with a certain beginning molecule shape.

### Thermochemistry

The impact of adding Cl element to chlorohydroquinone molecule is the primary goal of thermochemistry. The thermodynamic characteristics parameters associated with this chemical in the gas phase were calculated using DFT approach, B3LYP level of theory (method) with a 3-21G basis set, and are shown in Table 1 below. These thermodynamic possessions parameters include thermal energy (E), entropy (S), and molar heat capacity (Cv). These values of those variables are directly related to the temperatures that are being measured. Additionally, when temperatures improve, there is a rise in atomic oscillation and vibration.

The three equations produce the final formulas for calculating the components of physicochemical values observed by Gaussian. In equation (1), entropy S contributes from every component may be calculated using its partition function:[22]

$$S = R\left( \ln\left(q_t q_e q_r q_v e\right) + T\left(\frac{\partial \ln q}{\partial T}\right)_{\cdot V} \right) \quad (1)$$

The partition function may also be used to calculate the total internal thermal energy, which is denoted by E as shown in equation (2):

$$E = NK_B T^2 \left(\frac{\partial \ln q}{\partial T}\right)_V \quad (2)$$

**Table 1.** The influence Cl element to chlorohydroquinone molecule on the relevant thermodynamic coefficients at 298.15 K, and 1 atm Using the B3LYP level of theory (method) with a 3-21G basis set

| Calculation of parameters | Unit | 2-chlorobenzene-1,4-diol | 2,5-dichlorobenzene-1,4-diol | 2,3,5,6-tetrachlorobenzene-1,4-diol |
|---|---|---|---|---|
| E (Thermal) | kcal/mol | 66.979 | 61.672 | 51.112 |
| Cv | cal/mol.K | 29.802 | 33.494 | 40.916 |
| S | cal/mol.K | 86.838 | 93.464 | 107.516 |

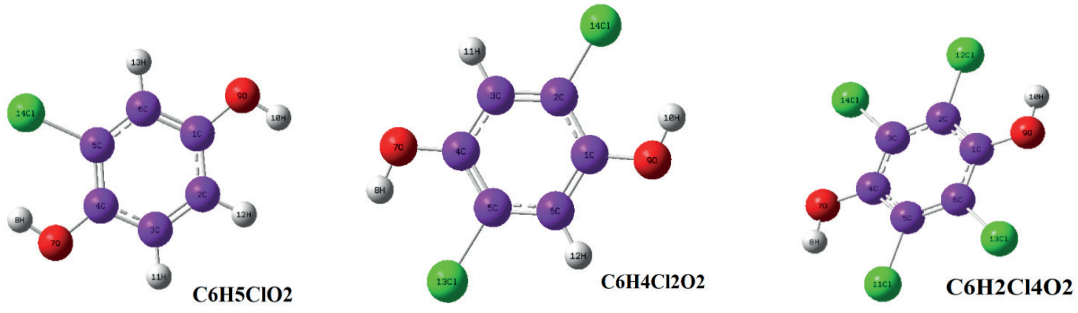


**Figure 2.** Geometry optimization with DFT method

and last equation (3), the energy may be put to use to measure the total heat capacity Cv:

$$Cv = \left(\frac{\partial E}{\partial T}\right)v \quad (3)$$

The ability to absorb heat and the temperature are completely related to one another.[23] The addition of chlorine (Cl) to a chlorohydroquinone molecule modifies its thermochemistry because it changes the structure and characteristics of the molecule. Adding a Cl atom may make the molecule more polar, which changes a lot of thermochemical things including bond energies, molecular vibrational, heat capacities, and heats of formation. which in turn affects its reactivity and interactions with other molecules as shown in Table 1.

## Computed electronic structure

Molecules have unique and various separate orbitals, which are distinct from the orbitals observed among atoms. The amount of energy that is different between the HOMO and LUMO states could be used to help identify the kind of molecule that it is. This energy is referred to as the band gaps (BGs).[24,25] In the current investigation, a wide variety of BG energy values have been analyzed and compared for each basis set (6-31G, 6-311G and 3-21G) for the compounds (2-chlorobenzene-1,4-diol, 2,5-dichlorobenzene-1,4-diol, and 2,3,5,6-tetrachlorobenzene-1,4-diol) with chemical formulas ($C_6H_5ClO_2$, $C_6H_4Cl_2O_2$, and $C_6H_2Cl_4O_2$), respectively. The following equations (4), and (5) illustrate the structure of the molecule's electron affinity (A), as well as its ionization potential:[26]

$$A = -E_{LUMO} \quad (4)$$

and

$$I = -E_{HOMO} \quad (5)$$

The following equation (6) was used to compute the value of the BG energy variable, which is represented by the symbol E:

$$\Delta E = E_{HOMO} - E_{LUMO} \quad (6)$$

This equation gives the basis for obtaining a theoretical calculation of the electronegativity (χ), hardness (η), and molecular softness (σ) as demonstrated in equations (7), (8), and (9):[24]

$$\chi = (I + A) / 2 \quad (7)$$

$$\eta = (I - A) / 2 \quad (8)$$

$$\sigma = 1/\eta \quad (9)$$

To calculate the values of Chemical potential (Pi), and dipole moment ($\mu$), as given in equations (10), and (11):[26]

$$Pi = -\chi \quad (10)$$

$$\mu = -(I+A)/2 \quad (11)$$

According to Table 2, the largest amount of BG energy that can be transferred between HUMO and LOMO in a 2-chlorobenzene-1,4-diol molecule is 5.46 eV when using a 6-31G basis set for the DFT technique, and 5.74 eV when using a 6-31G basis set for the Hartree-Fock method. There is seen small change energy gap. When using the DFT approach, the lowest BG to 2,5-dichlorobenzene-1,4-diol was determined at 5.33 eV when using the 6-311G basis set, whereas the largest BG was calculated at 6.93 eV when employing the Hartree-Fock method and same basis set as can be observed from Table 4. The final result for 2,3,5,6-tetrachlorobenzene-1,4-dio showed that the greatest BG energy was determined to be around 7.61 eV when the Hartree-Fock technique was used using the 6-31G basis set as has been shown in Table 6. Figure 3 displayed HOMO and LUMO energy for each title compound using HF and DFT method.

In the current investigation, the compounds 2-chlorobenzene-1,4-diol, 2,5-dichlorobenzene-1,4-diol, and 2,3,5,6-tetrachlorobenzene-1,4-diol) were found to have the (A), Electronegativity (χ), Chemical potential (Pi), and Dipole moment ($\mu$) with using the HF and DFT approach, as shown in Tables 3, 5, and 7. This finding suggested that the Cl compound had some influence on the results we obtained.

When the band gap energy is positive, it means that the LUMO is energetically situated higher than the HOMO. Because chlorine is a halogen with a high electronegativity, the value of electronegativity increased with compounds containing chlorine, as can be seen in the tables that are arranged according to electronegativity, and Cl makes a contribution to the electronegativity of the compound as a whole. in the present study, when evaluated as a whole, the electronegativity of the compounds contributes to an increase in the dipole moment of a molecule. In most cases, the dipole moment will grow as the electronegativity decreases.

The global reactivities are strongly linked to the corrosion resistance, chemical reactivity, stability, and inhibitor resistance of compounds. Compounds with higher hardness tend to have lower chemical

**Table 2.** BGs energy with various basis set for 2-chlorobenzene-1,4-diol

| Basis Set | DFT | | | HF | | |
|---|---|---|---|---|---|---|
| | HOMO (eV) | LUMO (eV) | Energy (eV) | HOMO (eV) | LUMO (eV) | Energy (eV) |
| 3-21G | -5.77 | -0.113 | 5.36 | -0.113 | -3.08 | 5.53 |
| 6-31G | -5.99 | -0.110 | 5.46 | -0.110 | -2.99 | 5.74 |
| 6-311G | -6.23 | -0.100 | 5.39 | -0.100 | -2.73 | 6.11 |

**Table 3.** Molecular parameters of 2-chlorobenzene-1,4-diol)

| Global reactivates | Unit | DFT | | | HF | | |
|---|---|---|---|---|---|---|---|
| | | 6-31G | 6-311G | 3-21G | 6-31G | 6-311G | 3-21G |
| Ionization potential (I) | eV | 5.99 | 5.99 | 6.23 | 8.62 | 8.74 | 8.84 |
| Electron affinity (A) | eV | 0.41 | 0.53 | 0.84 | 3.08 | 2.99 | 2.73 |
| Electronegativity (χ) | eV | 3.20 | 3.26 | 3.53 | 5.85 | 5.87 | 5.79 |
| Chemical potential (Pi) | eV | -3.20 | -3.26 | -3.53 | -5.85 | -5.87 | -5.79 |
| Molecular hardness (η) | eV | 2.79 | 2.73 | 2.69 | 2.79 | 2.87 | 3.05 |
| Molecular softness (σ) | $eV^{-1}$ | 0.35 | 0.36 | 0.37 | 0.35 | 0.34 | 0.32 |
| Dipole moment ($\mu$) | Debye | -2.20 | -3.26 | -3.53 | -5.85 | -5.87 | -5.79 |

**Table 4.** Energy BGs with various basis set for 2,5-dichlorobenzene-1,4-diol

| Basis Set | DFT | | | HF | | |
|---|---|---|---|---|---|---|
| | HOMO (eV) | LUMO (eV) | Energy (eV) | HOMO (eV) | LUMO (eV) | Energy (eV) |
| 3-21G | -6.63 | -0.81 | 5.82 | -9.09 | 2.58 | 6.42 |
| 6-31G | -6.31 | -0.89 | 5.41 | -9.11 | -2.53 | 6.58 |
| 6-311G | -6.55 | -1.22 | 5.33 | -9.22 | -2.28 | 6.93 |

**Table 5.** Molecular parameters of 2,5-dichlorobenzene-1,4-diol

| Global reactivates | Unit | DFT | | | HF | | |
|---|---|---|---|---|---|---|---|
| | | 6-31G | 6-311G | 3-21G | 6-31G | 6-311G | 3-21G |
| Ionization potential (I) | eV | 6.63 | 6.31 | 6.55 | 9.25 | -9.52 | - 7.07 |
| Electron affinity (A) | eV | 0.81 | 0.89 | 1.22 | 1.90 | 1.90 | -2.99 |
| Electronegativity ($\chi$) | eV | 3.72 | 3.60 | 3.89 | 5.57 | 5.71 | 5.03 |
| Chemical potential (Pi) | eV | -3.72 | -3.60 | 3-.89 | -5.57 | -5.71 | -5.03 |
| Molecular hardness ($\eta$) | eV | 2.91 | 2.70 | 2.66 | 3.67 | 3.87 | 2.04 |
| Molecular softness ($\sigma$) | $eV^{-1}$ | 0.26 | 0.27 | 0.25 | 0.27 | 0.25 | 0.49 |
| Dipole moment ($\mu$) | Debye | -3.72 | -3.60 | -3.89 | -9.25 | -9.52 | - 7.07 |

**Table 6.** Energy BGs with various bases set 2,3,5,6-tetrachlorobenzene-1,4-diol

| Basis Set | DFT | | | HF | | |
|---|---|---|---|---|---|---|
| | HOMO (eV) | LUMO (eV) | Energy (eV) | HOMO (eV) | LUMO (eV) | Energy (eV) |
| 3-21G | -6.53 | -1.63 | 4.89 | -9.25 | -1.90 | 7.34 |
| 6-31G | -7.07 | -2.99 | 4.08 | -9.52 | -1.90 | 7.61 |
| 6-311G | -6.80 | -1.90 | 4.89 | -7.07 | -2.99 | 4.08 |

**Table 7.** Molecular parameters of 2,3,5,6-tetrachlorobenzene-1,4-diol

| Global reactivates | Unit | DFT | | | HF | | |
|---|---|---|---|---|---|---|---|
| | | 6-31G | 6-311G | 3-21G | 6-31G | 6-311G | 3-21G |
| Ionization potential (I) | eV | 6.53 | 7.07 | 6.80 | 9.25 | 9.52 | 7.07 |
| Electron affinity (A) | eV | 1.63 | 2.99 | 1.90 | 1.90 | 1.90 | 2.99 |
| Electronegativity ($\chi$) | eV | 4.08 | 5.03 | 4.35 | 5.57 | 5.71 | 5.03 |
| Chemical potential (Pi) | eV | -4.08 | -5.03 | -4.35 | -5.57 | -5.71 | -5.03 |
| Molecular hardness ($\eta$) | eV | 2.45 | 2.04 | 2.45 | 3.87 | 2.04 | 3.8 |
| Molecular softness ($\sigma$) | $eV^{-1}$ | 0.40 | 0.49 | 0.40 | 0.25 | 0.49 | 0.19 |
| Dipole moment ($\mu$) | Debye | 4.08 | 5.03 | 4.35 | 5.71 | 5.03 | 5.71 |

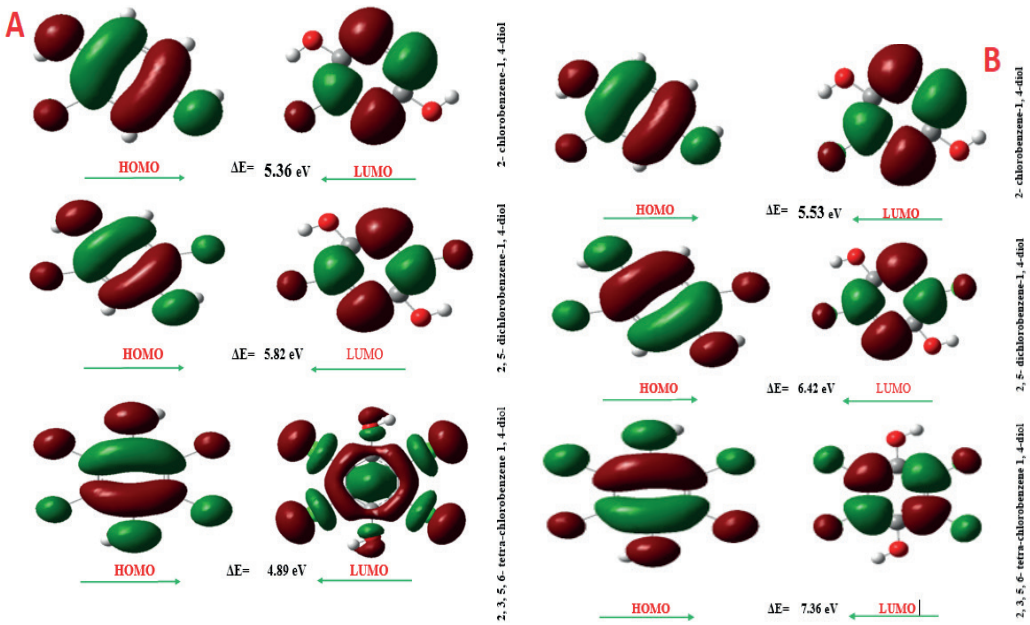


**Figure 3a.** The FMO diagram for title compounds using 3-21G basis set, (A) DFT, and (B) HF approach

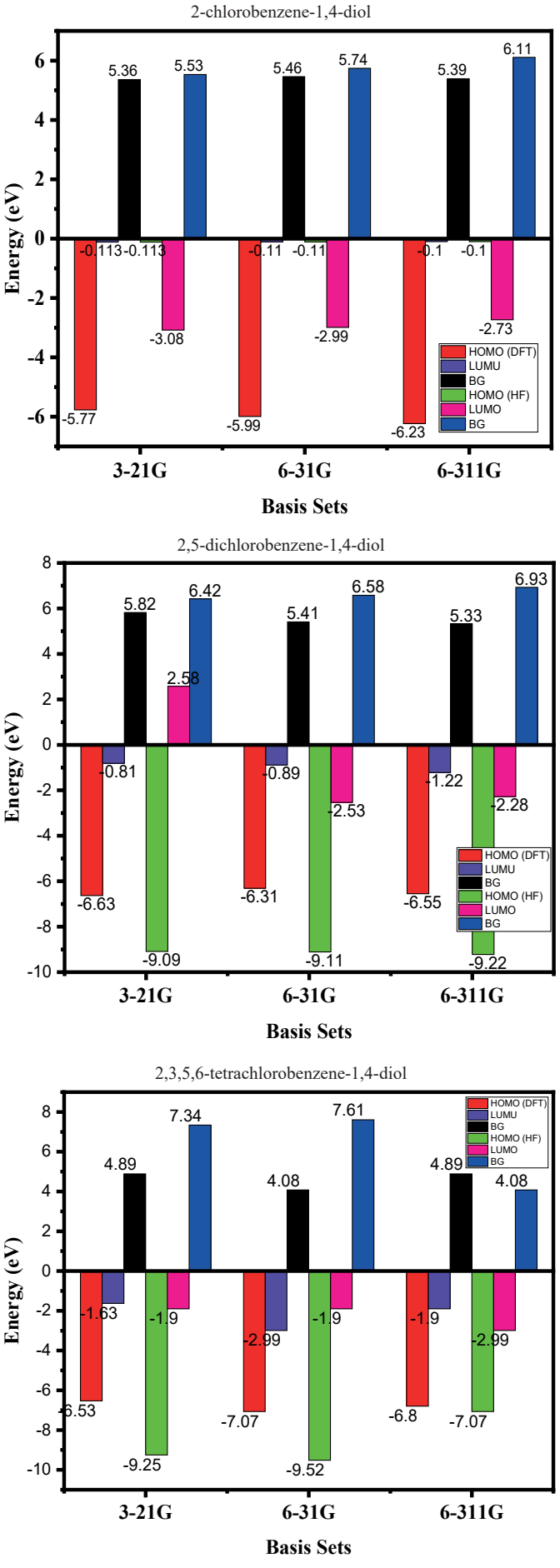


**Figure 3b.** HOMO, LUMO, and BG energy representation for the title compounds

reactivity and greater chemical stability when their HOMO-LUMO energy gaps are bigger. The energy gap is closely associated to the molecular hardness data from each table. Because it takes more energy to break stronger bonds, molecules with these bond strengths are less likely to respond. Based on this data, 2,3,5,6-tetrachlorobenzene-1,4-diol had the narrowest energy gap (4.89, 4.08, and 4.89 eV) in DFT approach. Here is conclude that, according energy gap the 2,3,5,6-tetrachlorobenzene-1,4-diol compound more reactive than two other compounds. The evidence presented here suggests that the element Cl has a chemical influence on global reactivates when the compound chlorohydroquinone is used.

## UV spectrum

To investigate the adsorption characteristics of compound surfaces, a variety of physicochemical techniques are used UV spectroscopy is a typical method for identifying the structures of compounds, as well as doing qualitative and quantitative analyses of the compounds individually.[25,27] In the current investigation, the DFT technique and the B3LYP level of theory, and TD-SCF method to calculate UV-spectroscopy were used, and the basis set ranged from 3-21G. However, the theoretical findings of UV spectroscopy performed on 2-chlorobenzene-1,4-diol, 2,5-dichlorobenzene-1,4-diol, and 2,3,5,6-tetrachlorobenzene-1,4-diol, as shown in Figure 4. Additionally, the maximum excitation energy was explored at a wavelength of 258.16 nm, 264.15 nm, and 267.07 nm the oscillator strength was evaluated at 0.0747, 0.0003, and 0.116 UV Spectroscopy.

The highest excitation energy of 2,3,5,6- tetrachlorobenzene-1,4-diol was investigated in the past at wavelengths ranging from 328 to 354 nanometers. Compared to our theoretical results, this result agrees with what we found.[26]

## Electronic DOS

In a quantum mechanical system, the density of states (or DOS) of an electronic device is a measurement that determines how densely electrons are "packed" in various energy levels.[28-29] In this research work, we investigated the DOS of 2-chlorobenzene-1,4-diol, 2,5-dichlorobenzene-1,4-diol, and 2,3,5,6-tetrachlorobenzene-1,4-diol using DFT with a 3-21G basis set. However, equation (14) demonstrates that it is helpful to use the formula to determine the DOS as a function of energy levels:[30-32]

$$DOS(E) = \Sigma g(E - \varepsilon i) \quad (14)$$

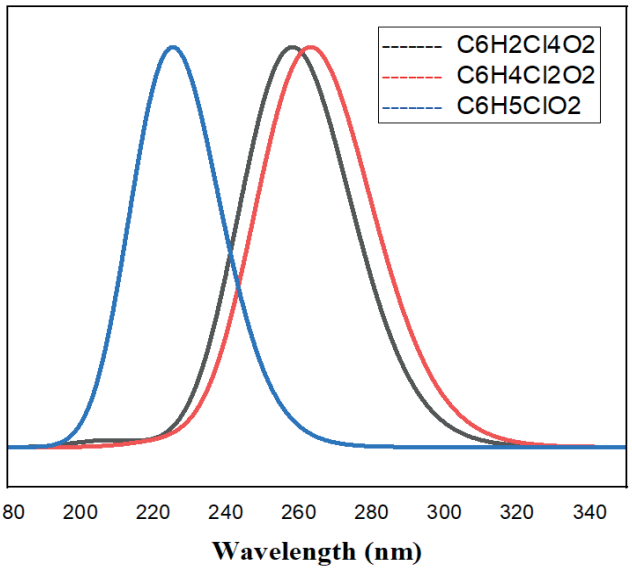


**Figure 4.** UV Spectroscopy with RB3LYP/ TD-SCF with 3-21G basis set, and DFT method

where E = total electron energy, g is a Gaussian function with a constant FWHM = 0.3, and The value εi denotes the energy of the ith orbitals. According to Figure 5 a,b and c, with increasing Cl compound, the greatest peak of DOS that was observed for 2,5-dichlorobenzene-1,4-diol and 2,3,5,6-tetrachlorobenzene-1,4-diol was around 15 eV, and the energy range ranged from -20 eV to 20 eV. There is a clear association between the drop in BG energy for DOS when there are 4 Cl (4.89 eV): the rise in electronegativity (4.35 eV), the decrease in molecular softness (0.40 $eV^{-1}$), and the decrease in molecular hardness for (2.45 eV).

## Potential energy surfaces (PES)

The potential energy map (PEM) is an extremely important component in the process of describing the arrangement of the structural components of the molecule. The important function of those potential energy surface (PES) characteristics, as well as in the explanations of the orientation of the electrons in the complicated molecules that are being investigated. The electronic density (ρ) and the electrostatic potential map are both components of the electrostatic potential (EP), ($PE_{map} = \rho + EP$ ).[33-35] The following equation 15 may be used in order to investigate the evolution of the electromagnetic field (ESP) surrounding molecules in space.[36]

$$\mathbb{V}_{(r)} = \sum_{A} \frac{Z_A}{R_A - r} - \int \frac{\rho(r)\,dU}{U - r} \qquad (15)$$

$Z_A$ is a representation of a nuclear charge that is located at RA, and ρ(r) is a representation of the electronic density. Potential, which is represented by the symbol V, is a function of distance, which is represented by the symbol (r). The MEP region was selected to have one of the following color schemes: red zone is the rich electronic charge, blue zone: is poor electronic charge density, and rich positive (+) charge, light blue area: is the zone that is somewhat lacking in electrons, yellow area: is a area that is a bit rich in electrons density, and green: neutral.[36-38]

The charge distribution on compounds is shown in Table 8, as seen above. The Mulliken density analysis, often known as the charge distribution, is a method that is frequently used for assessing the amount of inhibitor absorption. According to the findings of a large number of studies, the presence of negatively charged heteroatoms improves the capacity of donor-acceptor processes to absorb on the surface of metallic elements. In light of this information, naphthalene has a significant inhibitory impact due to a greater negative charge located in the center of the molecule.

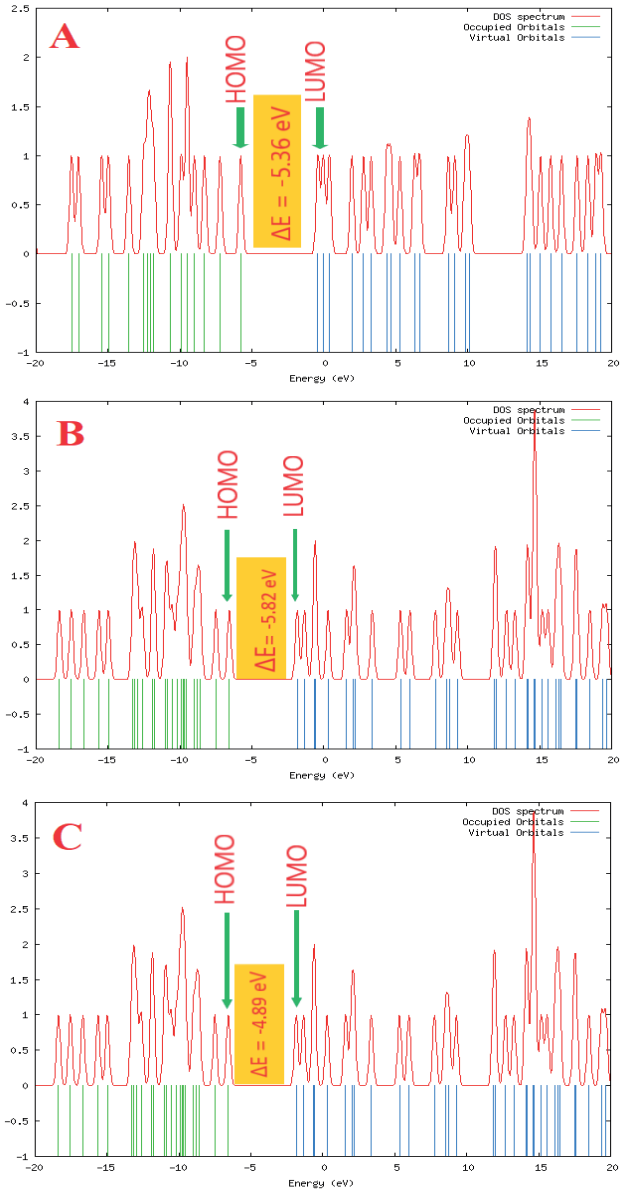


**Figure 5.** Electronic DOS Using the B3LYP level of theory (method) with a 3-21G basis set for: A) 2- chlorobenzene-1,4-diol, B) 2, 5-dichlorobenzene-1,4-diol, and C) 2,3,5,6-tetrachlorobenzene-1,4-diol

**Table 8.** Charge is distributed throughout the atoms in this model using the B3LYP level of theory (method) with a 3-21G basis set

| 2- chlorobenzene-1,4-diol | | 2,5-dichlorobenzene-1,4-diol | | 2,3,5,6- tetrachlorobenzene-1,4-diol | |
|---|---|---|---|---|---|
| Atoms | Charge distribution | Atoms | Charge distribution | Atoms | Charge distribution |
| 1 - C | 0.289231 | 1 C | 0.377162 | 1 C | 0.400815 |
| 2 - C | -0.217582 | 2 C | -0.377162 | 2 C | -0.339993 |
| 3 - C | -0.177747 | 3 C | -0.132526 | 3 C | -0.317181 |
| 4 - C | 0.320977 | 4 C | 0.330704 | 4 C | 0.402611 |
| 5 - C | -0.285728 | 5 C | -0.286971 | 5 C | -0.250324 |
| 6 - C | -0.161518 | 6 C | -0.154615 | 6 C | -0.341878 |
| 7 - O | -0.599244 | 7 O | -0.595711 | 7 O | -0.571402 |
| 8 - H | 0.369304 | 8 H | 0.373508 | 8 H | 0.380271 |
| 9 - O | -0.600037 | 9 O | -0.592472 | 9 O | -0.568128 |
| 10 - H | 0.357342 | 10 H | 0.370713 | 10 H | 0.377863 |
| 11 - H | 0.216827 | 11 H | 0.240074 | 11 Cl | 0.128830 |
| 12 - H | 0.187135 | 12 H | 0.244153 | 12 Cl | 0.211761 |
| 13 - H | 0.233370 | 13 Cl | 0.079744 | 13 Cl | 0.249827 |
| 14 - Cl | 0.067670 | 14 Cl | 0.164566 | 14 Cl | 0.236928 |

The density of electrons (ρ) is the number of electrons per unit volume in a particular area of space and measures the possibility of their particle position. In physics, electrostatic potential is defined as the momentum of attraction between a positive unit charge and a collection of electrons or molecules [39-40].

As can be shown in Figure 6, the potential energy of chlorohydroquinone has been studied using B3LYP, 3-21G basis set, and the DFT method. As a result of this effect, our compounds (chlorohydroquinone) remove (push) electrons from their surroundings and become electron-poor (the blue portion). The red color surrounding the molecule is because all electrons in the molecule surround it. Figure 6 shows that adding Cl increases and decreases electron density when the color is blue in the range of -9.595 $e^{-2}$ to 9.595 $e^{-2}$, -7.748 $e^{-2}$ to 7.748 $e^{-2}$, and -8.884 $e^{-2}$ to 8.884 $e^{-2}$. The electronegative potential of chlorine is greater than that of either carbon or hydrogen atom. As a result, as the concentration of the Cl atom increased, the electrons moved toward the oxygen, leaving behind a blue tint that indicated an electron deficit. Finally, the O-H groups are characterized by a high concentration of blue, a low electronic charge density, and a high positive (+) charge as seen Figure 6.[33]

## Nuclear Magnetic Resonance (NMR) Spectroscopy

NMR spectroscopy, or nuclear magnetic resonance, is a modern analysis method. It may reveal the atomic structure of a sample's molecules. Phase shifts, structural and configurational changes, solubility, and diffusion potential are all things that NMR spectroscopy can identify in addition to the chemical structure.[41]

Increasing the amount of Cl in a molecule causes a change in the NMR chemical shift values, as shown in Table 9 for method A) 2-chlorobenzene-1,4-diol, method B) 2-chlorobenzene-1,5-diol, and method C) 2-chlorobenzene-1,4,6-tetrachlorobenzene-1,4-diol.

The vertical excitation has been calculated using density functional theory (DFT) at the equilibrium geometry of the ground state. At a single spin location, we determine the DFT. Table 10 below displays the optimal form at the ground state energy E(RB3LYP). Table 11 below shows that the optimized form at ground state energy decreased from -837.98 to -2210.13 a.u, and dipole moment from 3.137 to 0.3747 Dy.

## Reduced density gradient (RDG) Scatter

Some examples of innovative approaches that are employed for the aim of exploring weak intermolecular interactions include procedures known as reduced density gradient (RDG) procedures. Additionally, the theory describes the molecule's stable structure, molecular recognition, physical and chemical characteristics, and biological activity. Small intramolecular or intermolecular forces influencing molecular stability may be revealed by RDG estimates. Differentiating between hydrogen bonds, steric repulsion, and van der Waals interactions in molecules and tiny particles is possible using the RDG method. This concept may be stated mathematically using the

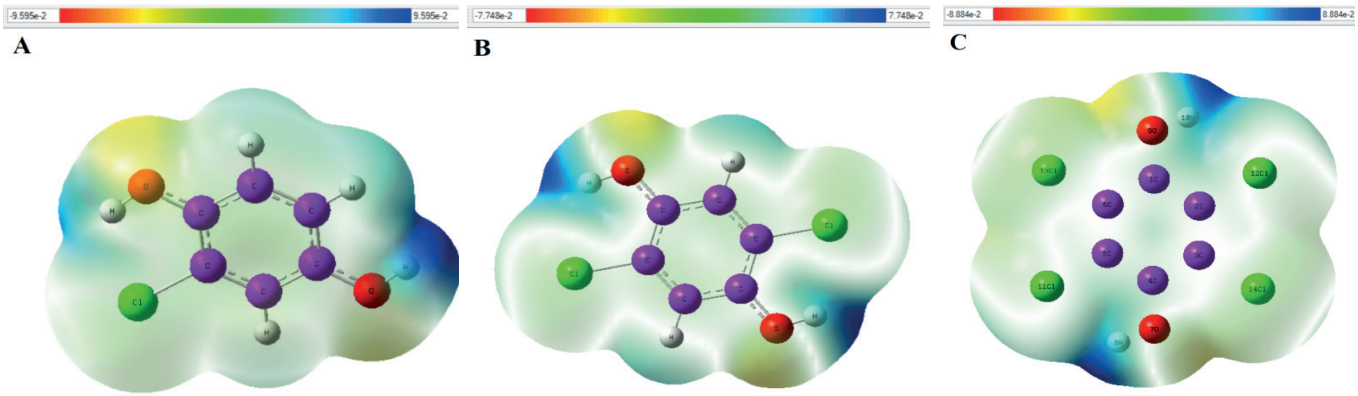


**Figure 6.** Potential energy maps (PEM) for: A) 2- chlorobenzene-1,4-diol, B) 2,5-dichlorobenzene-1,4-diol, and C) 2,3,5,6- tetrachlorobenzene-1,4-diol with 3-21G basis set, and B3LYP/DFT method.

**Table 9.** NMR Chemical Shielding, using the B3LYP level of theory (method) with a 3-21G basis set

| a) Method | Shielding (ppm) | b) Method | Shielding (ppm) | c) Method | Shielding (ppm) |
|---|---|---|---|---|---|
| 1-C | 66.09 | 1-C | 112.09 | 8-H | 27.18 |
| 14-Cl | 802.72 | 14-Cl | 952.49 | 10-H | 27.35 |
| 2-C | 98.43 | 2-C | 119.53 | 1-C | 72.77 |
| 11-H | 26.21 | 11-H | 26.15 | 4-C | 74.48 |
| 3-C | 98.97 | 3-C | 132.59 | 5-C | 82.21 |
| 12-H | 26.44 | 12-H | 26.08 | 3-C | 82.21 |
| 4-C | 72.26 | 4-C | 113.90 | 2-C | 88.83 |
| 13-H | 26.38 | 13-Cl | 912.54 | 6-C | 90.05 |
| 5-C | 82.53 | 5-C | 111.71 | 7-O | 216.14 |
| 8-H | 27.91 | 8-H | 28.78 | 9-O | 217.06 |
| 7-O | 231.07 | 7-O | 255.09 | 11-Cl | 739.67 |
| 6-C | 100.99 | 6-C | 135.27 | 14-Cl | 756.09 |
| 9-O | 221.01 | 9-O | 253.31 | 13-Cl | 756.09 |
| 10-H | 28.18 | 10-H | 27.98 | 12-Cl | 797.11 |

**Table 10.** Calculation method of NMR, using with B3LYP level of theory (method) with a 3-21G basis set

| Parameters | Methods |
|---|---|
| Calculation Type | SP |
| Calculation Method | RB3LYP |
| Basis Set | 3-21G |
| Charge | 0 |
| Degeneracy Tolerance | 0.05 |
| Spin | Singlet |

following equation (16):[42-44]

$$RDG(r) = \frac{1|\nabla\rho(r)|}{2\left(3\pi r^2\right)^{\frac{1}{3}}\rho^{\frac{4}{3}}(r)} \qquad (16)$$

The a high level of RDG value indicates strong attraction, and rich electron connections, while the low-density RDG value confirms regions with low electron concentration, which are responsible for weak interactions. Interactions may be categorized into three groups using the equation (λ2)ρ: 1st : The attraction, which may be either a hydrogen bond or a dipole–dipole, is distinguished by the presence of negative (-) sign values (λ2)ρ. 2nd : There is a correlation between values that are near to zero and weak contacts, also known as van der Waals interactions. 3rd : This interaction is of a strong repulsion kind, and it is proven by the presence of large and positive (+) values of the sign (λ2)ρ. The red color represents strong interactions, the green hue represents van der Waals interactions, and the blue color represents strong hydrogen bond interactions, as seen in Figure 7.[42]

## CONCLUSION

In the current investigation, many aspects of the physical and chemical behavior of 2-chlorobenzene-1,4-diol, 2,5-dichlorobenzene-1,4-diol, and 2,3,5,6-tetrachlorobenzene-1,4-diol) compound with chemical formulas ($C_6H_5ClO_2$), ($C_6H_4Cl_2O_2$), and ($C_6H_2Cl_4O_2$) have been examined. These aspects include (HOMO, LUMO, DOS, and UV spectroscopy), and the Gaussian 5.0 program, which includes DFT and the Hartree-Fock technique, has been used. Based on this data, 2,3,5,6-tetrachlorobenzene-1,4-diol compound had the narrowest energy gap (4.89, 4.08, and 4.89 eV) in DFT approach. Here is conclude that, according energy gap the 2,3,5,6-tetrachlorobenzene-1,4-diol compound more reactive than two other compounds. The higher electronegativity of the compounds is partially due to the presence of chlorine. The majority of the time, the dipole moment will increase as the electronegativity goes down. The maximal excitation energy was investigated at 258.16, 264.15, and 267.07 nm. Oscillator strength was 0.0747, 0.0003, and 0.116 UV Spectroscopy.

There is a direct correlation between the reduction in BG energy for DOS when there are 4 Cl 4.89 eV and the following: the increase in electronegativity (4.35 eV), the decrease in molecular softness (0.40 eV-1), and the decrease in molecular hardness for (2.45 eV). This observation revealed that the Cl in the compound had some impact on our findings because of the affected electronegativity, electron affinity, and dipole moment of the Cl element. As a result of PES, as the concentration of Cl atom increased, a blue tint indicated an electron deficit. Finally, the chemical shift measurements of the (H, O, C, and Cl) molecule are completed in an NMR shielding. According RDG result, the red color represents strong interactions, the green hue represents van der Waals interactions, and the blue color represents strong hydrogen bond interactions.

## ACKNOWLEDGEMENTS

We would like to thank the heads of the physics departments at Halabja University for their support.

**Table 11.** NMR calculation

| Parameters | Unit | Method A | Method B | Method C |
|---|---|---|---|---|
| Dipole Moment | (Dy) | 3.137 | 0.2933 | 0.3747 |
| E(RB3LYP) | (a.u.) | -837.98 | -1295.37 | -2210.13 |

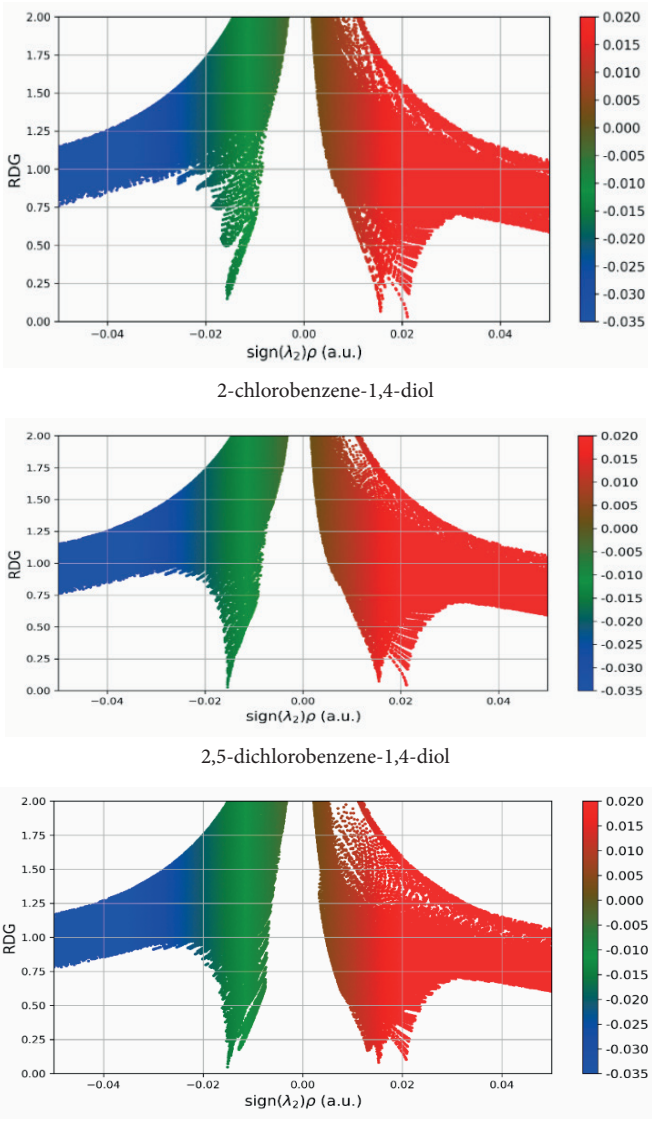


**Figure 7.** Reduced density gradient (RDG) scatter B3LYP level of theory (method) with a 3-21G basis set

## CONFLICT OF INTEREST

The authors have no conflicts of interest to declare that are relevant to the content of this article.

## ORCID IDS

Rebaz Obaid Kareem: https://orcid.org/0000-0001-6273-1309
Othman Abdulrahman Hamad: https://orcid.org/0000-0001-8170-9094
Bast Ahmad: https://orcid.org/0009-0004-3774-633X
Hanifi Kebiroglu: https://orcid.org/0000-0002-6764-3364

## REFERENCES

1. Olaniran AO, Igbinosa EO. Chlorophenols and other related derivatives of environmental concern: properties, distribution and microbial degradation processes. Chemosphere. 2011;83(10):1297–1306. https://doi.org/10.1016/j.chemosphere.2011.04.009.

2. Schmid S, Krajnik P, Quint R, Solar S. Degradation of monochlorophenols by γ-irradiation. Radiat Phys Chem. 1997;50(5):493–502. https://doi.org/10.1016/S0969-806X(97)00075-3.
3. Zhang J, Liu D, Bian W, Chen X. Degradation of 2, 4-dichorophenol by pulsed high voltage discharge in water. Desalination. 2012;304:49–56. https://doi.org/10.1016/j.desal.2012.01.027.
4. Kwan C, Chu W. A study of the reaction mechanisms of the degradation of 2, 4-dichlorophenoxyacetic acid by oxalate-mediated photooxidation. Water Res. 2004;38(19):4213–4221. https://doi.org/10.1016/j.watres.2004.06.033.
5. Rossi A, Tournebize A, Boule P. Phototransformation of chlorohydroquinone in aqueous solution. J Photochem Photobiol Chem. 1995;85(3):213–216. https://doi.org/10.1016/1010-6030(94)03908-D.
6. Wang Y, Shen Z, Li Y, Niu J. Electrochemical properties of the erbium–chitosan–fluorine–modified PbO2 electrode for the degradation of 2, 4-dichlorophenol in aqueous solution. Chemosphere. 2010;79(10):987–996. https://doi.org/10.1016/j.chemosphere.2010.03.029.
7. Ding S, Tan P, Wen J, Li T, Wang W. Quantification of 2-chlorohydroquinone based on interaction between N-doped carbon quantum dots probe and photolysis products in fluorescence system. Sci Total Environ. 2022;814:152745. https://doi.org/10.1016/j.scitotenv.2021.152745.
8. Asgari G, Sidmohammadi A, Rahmani AR, Samargandi MR, Faraji H. Efficient decomposition of pentachlorophenol by a high photon flux UV/sodium hydrosulfite: Kinetics, intermediates and associated transformation pathway. Optik (Stuttg). 2020;218:164981. https://doi.org/10.1016/j.ijleo.2020.164981.
9. Liu Y, Zhao Y, Wang J. Activation of peroxydisulfate by a novel Cu0-Cu2O@CNTs composite for 2, 4-dichlorophenol degradation. Sci Total Environ. 2021;754:141883. https://doi.org/10.1016/j.scitotenv.2020.141883.
10. Chaliha S, Bhattacharyya KG. Wet oxidative method for removal of 2, 4, 6-trichlorophenol in water using Fe (III), Co (II), Ni (II) supported MCM41 catalysts. J Haz Mat. 2008;150(3):728–736. https://doi.org/10.1016/j.jhazmat.2007.05.039.
11. Rao N, Dubey A, Mohanty S, Khare P, Jain R, Kaul S. Photocatalytic degradation of 2-chlorophenol: a study of kinetics, intermediates and biodegradability. J Hazard Mater. 2003;101(3):301–314. https://doi.org/10.1016/S0304-3894(03)00180-8.
12. Zada A, Qu Y, Ali S, Sun N, Lu H, Yan R, Zhang X, Jing L. Improved visible-light activities for degrading pollutants on TiO2/g-C3N4 nanocomposites by decorating SPR Au nanoparticles and 2, 4-dichlorophenol decomposition path. J Hazard Mater. 2018;342:715–723. https://doi.org/10.1016/j.jhazmat.2017.09.005.
13. Akai N, Kudoh S, Nakata M. Hydrogen-atom migration and Wolff rearrangement in photolysis of chlorohydroquinone to produce p-benzoquinone and 3-hydroxy-2, 4-cyclopentadiene-1-ylidenemethanone. J Photochem Photobiol Chem. 2005;169(1):47–55. https://doi.org/10.1016/j.jphotochem.2004.05.033.
14. Manurkar N, More S, Mulani K, Ganjave N, Chavan N. Thermotropic liquid crystalline polyesters derived from 2-chloro hydroquinone. J Chem Sci. 2017;129(9):1461–1468. https://doi.org/10.1007/s12039-017-1342-y.
15. Sulfab Y, Al-Sogair FM. Kinetics and mechanism of reduction of 3, 9-diethyl-4, 8-diaza-3, 8-undeca-2, 10-dionedioximatocopper (III) complex by p-methoxyphenol, 1, 2-dihydroxybenzene, 1, 4-dihydroxybenzene and some of its derivatives in aqueous acidic solutions. Polyhedron. 2004;23(4):583–588. https://doi.org/10.1016/j.poly.2003.10.011.
16. Brillas E, Calpe JC, Casado J. Mineralization of 2, 4-D by advanced electrochemical oxidation processes. Water Res. 2000;34(8):2253–2262. https://doi.org/10.1016/S0043-1354(99)00396-6.
17. Hariharan V, Prabu NPS, Mohan MM. Design, synthesis and analysis of chlorohydroquinone derivatives—liquid crystalline complexes. Mol Cryst Liq Cryst (Phila Pa). 2014;593(1):78–92. https://doi.org/10.1080/15421406.2013.867225.
18. Kareem RO, Kebiroglu H, Hamad OA, Kaygili O, Bulut N. Epinephrine Compound: Unveiling its Optical and Thermochemical Properties Via Quantum Computation Methods. https://doi.org/10.2139/ssrn.4603446.
19. Nazem Qader I, Mohammad A, Azeez YH, Agid RS, Hassan HS, Al-Nabawi SHM. Chemical structural and vibrational analysis of potassium acetate: a density function theory study. J Phys Chem Func Mat. 2(1):23–25.
20. Etkeser Aktaş A, Omer R, Koparir M. Synthesis, characterization and theoretical anti-corrosion study for substitute thiazole contained cyclobutane ring. Journal of Physical Chemistry and Functional Materials. 2022;5(1):111–120. https://doi.org/10.54565/jphcfum.1121687.
21. Hekim S, Azeez YH, Akpinar S. The theoretical investigation of the HOMO, LUMO energies and chemical reactivity of C9H12 and C7F3NH5Cl molecules. Journal of Physical Chemistry and Functional Materials. 2019;2(1):29–31.
22. Ochterski JW. Thermochemistry in Gaussian. Wallingford: Gaussian Inc., 2000 (updated 2022). https://gaussian.com/wp-content/uploads/dl/thermo.pdf [accessed 25 March 2024].
23. Ganiev I, Khodzhanazarov KM, Khodzhaev F, Eshov B. Heat Capacity and Thermodynamic Functions of Sodium-Alloyed Lead Babbitt BNa (PbSb15Sn10Na). Russ J Phys Chem A Focus Chem. 2023;97(4):550–555. https://doi.org/10.1134/S0036024423040106.
24. Shahab H, Husain Y. Theoretical Study for Chemical Reactivity Descriptors of Tetrathiafulvalene in gas phase and solvent phases based on Density Functional Theory. Passer Journal of Basic and Applied Sciences. 2021;3(2):167–173. https://doi.org/10.24271/psr.28.
25. Pakhnutova EA, Slizhov YG. Adsorption of organic compounds on the surfaces of silicas with grafted acetoacet ether groups saturated with transition metal Ions. Russ J Phys Chem A Focus Chem. 2023;97(2):384–391. https://doi.org/10.1134/S003602442302019X.
26. Wang Y-J, Ho Y-S, Chu S-W, Lien H-J, Liu T-H, Lin J-K. Induction of glutathione depletion, p53 protein accumulation and cellular transformation by tetrachlorohydroquinone, a toxic metabolite of pentachlorophenol. Chem Biol Interact. 1997;105(1):1–16. https://doi.org/10.1016/S0009-2797(97)00023-9.
27. Hamad OA, Kareem RO, Omer PK. Recent developments in synthesize, properties, characterization, and application of phthalocyanine and metal phthalocyanine. J Chem Rev. 2024;6(1):39–75. https://doi.org/10.48309/jcr.2024.412899.1250.
28. Kareem RO, Kaygili O, Ates T, Bulut N, Koytepe S, Kuruçay A, Ercan F, Ercan I. Experimental and theoretical characterization of Bi-based hydroxyapatites doped with Ce. Ceram Int. 2022;48(22):33440–33454. https://doi.org/10.1016/j.ceramint.2022.07.287.
29. Korkmaz AA, Ahmed LO, Kareem RO, Kebiroglu H, Ates T, Bulut N, Kaygili O, Ates B. Theoretical and experimental characterization of Sn-based hydroxyapatites doped with Bi. Journal of the Australian Ceramic Society. 2022;58(3):803–815. https://doi.org/10.1007/s41779-022-00730-5.
30. İsen F, Kaygili O, Bulut N, Ates T, Osmanlıoğlu F, Keser S, Tatar B, Özcan İ, Ates B, Ercan F, et al. Experimental and theoretical characterization of Dy-doped hydroxyapatites. Journal of the Australian Ceramic Society. 2023;59(4):849–864. https://doi.org/10.1007/s41779-023-00878-8.
31. Kareem RO. Synthesis and Characterization Of Bismuth-Based Hydroxyapatites Doped With Cerium. MSc Thesis, Firat University, Türkiye, 2023.
32. Bulut N, Kaygili O, Hssain AH, Dorozhkin SV, Abdelghani B, Orek C, Kebiroglu H, Ates T, Kareem RO. Mg-Dopant Effects on Band Structures of Zn-Based Hydroxyapatites: A Theoretical Study. Indian J Sci. 2023;47(5-6):1843–1859. https://doi.org/10.1007/s40995-023-01531-6.
33. Nasidi II, Kaygili O, Majid A, Bulut N, Alkhedher M, ElDin SM. Halogen Doping to Control the Band Gap of Ascorbic Acid: A Theoretical Study. ACS Omega. 2022;7(48):44390–44397. https://doi.org/10.1021/acsomega.2c06075.
34. Hamad O, Obaid Kareem R, Kaygili O; HAMAD. O.; KAREEM, R. O.; Kaygili, O., Density Function Theory Study of the Physicochemical Characteristics of 2-nitrophenol. Journal of Physical Chemistry and Functional Materials. 2023;6(1):70–76. https://doi.org/10.54565/jphcfum.1273771.
35. Sadykov N, Petrova YA, Pilipenko I, Khrabrov R, Skryabin S. Effect of a Geometric Potential on the Eigenfunction and Eigenvalue of the Energy of State in a Twisted Graphene Nanoribbon. Russ J Phys Chem A Focus Chem. 2023;97(2):367–372. https://doi.org/10.1134/S003602442302022X.
36. Omer RA, Ahmed LO, Koparir M, Koparir P. Theoretical analysis of the reactivity of chloroquine and hydroxychloroquine. Ind J Chem. 2020;59A:1828–1834.
37. Jamalis J, Sebastian S, Margreat SS, Subashini K, Ramalingam S, Al-Maqtari HM, Periandy S, Xavier S. Synthesis, spectral characterization (FT-IR, FT-Raman and NMR) and Quantum computational analysis of (E)-1-(4-Bromophenyl)-3-(5-bromothiophen-2-yl) prop2-en-1-one. Chemical Data Collections. 2020;28:100415. https://doi.org/10.1016/j.cdc.2020.100415.

38. Kebiroğlu MH, Kareem RO, Hamad OA. Investigation of electronic and spectroscopic properties of phosphosilicate glass molecule (BioGlass 45S5) and Ti-BioGlass 45S5 by quantum programming. J Chem Lett. 2023;4:200–210. https://doi.org/10.22034/jchemlett.2024.416584.1138.
39. Zhelavskaya IS, Shprits YY, Spasojevic M. Reconstruction of plasma electron density from satellite measurements via artificial neural networks. In: Camporeale E, Wing S, Johnson JR (editors), Machine learning techniques for space weather. Elsevier; 2018. pp. 301–327. https://doi.org/10.1016/B978-0-12-811788-0.00012-3.
40. Bort JA, Rusca JB (editors). Theoretical and computational chemistry: foundations, methods and techniques Vol. 11. Castelló de la Plana: Publicacions de la Universitat Jaume I; 2007.
41. Walkare A, Solanki BS, Singh H, Sheorey T. Design and analysis of extrusion-compression molding setup for processing of glass fiber reinforced polypropylene composites. Mater Today Proc. 2023;72:3017–3022. https://doi.org/10.1016/j.matpr.2022.08.270.
42. Akman F, Demirpolat A, Kazachenko AS, Kazachenko AS, Issaoui N, Al-Dossary O. Molecular structure, electronic properties, reactivity (ELF, LOL, and Fukui), and NCI-RDG studies of the binary mixture of water and essential oil of phlomis Bruguieri. Molecules. 2023;28(6):2684. https://doi.org/10.3390/molecules28062684.
43. Domingo LR, Aurell MJ, Pérez P, Contreras R. Quantitative characterization of the global electrophilicity power of common diene/dienophile pairs in Diels–Alder reactions. Tetrahedron. 2002;58(22):4417–4423. https://doi.org/10.1016/S0040-4020(02)00410-6.
44. Asif M, Sajid H, Ayub K, Gilani MA, Anwar N, Mahmood T. Therapeutic potential of oxo-triarylmethyl (oxTAM) as a targeted drug delivery system for nitrosourea and fluorouracil anticancer drugs; A first principles insight. J Mol Graph Model. 2023;122:108469. https://doi.org/10.1016/j.jmgm.2023.108469.